Int. J. Electrochem. Sci., 16 **(2021)** Article Number: 21118, doi: 10.20964/2021.11.07

International Journal of
ELECTROCHEMICAL
SCIENCE
www.electrochemsci.org

Joint Dynamic Strategy of Bayesian Regularized Back Propagation Neural Network with Strong Robustness - Extended Kalman Filtering for the Battery State-of-Charge Prediction

Yifen Hu[1]*·Yixing Zhang*[2]*·Shunli Wang*[2]*·Wenhua Xu*[2] *·Yongcun Fan2·Yuyang Liu*[2]

[1] School of Automotive and Mechanical-electronic Engineering , Xinyang Vocational and Technical College, Xinyang 464000, China
[2] School of Information Engineering, Southwest University of Science and Technology, Mianyang, 621010, China
[*]E-mail: 497420789@qq.com

Received: 3 July 2021 / *Accepted:* 25 August 2021 / *Published:* 10 October 2021

Accurate estimation of the state of charge plays an important role in real-time monitoring and safety control of lithium-ion batteries. In practical application, the use of lithium-ion battery will face different sudden noise. Extended Kalman filtering (EKF) is deficient in this kind of processing, so this paper combines EKF with Bayesian regularized backpropagation neural network, and uses dynamic strategy to implement two algorithms to improve the accuracy and speed. Experimental results show that the joint algorithm has a stable effect and a good tracking effect under sudden noise conditions. Compared with the extended Kalman filtering algorithm, the average error of the algorithm in the capacity test is reduced by 0.797%, and the maximum error is reduced by 2.651%. In the dynamic stress test and the pulse test, the average error was reduced by 0.2683% and 0.3919%, and the maximum error was reduced by 7.195% and 7.769%, respectively. It is verified that the algorithm combining the extended Kalman filtering and the back propagation neural network has high accuracy in the estimation of the state of charge of the lithium-ion battery under sudden events.

Keywords: Sudden noise; Dynamic programming; BP neural network; Real-time; Bayesian regularized;

1. INTRODUCTION

In the modern world, energy security and green energy have always been the focus of attention [1, 2]. It is a necessary way for economy and environmental protection to replace traditional fossil fuels with new energy [3-6]. Due to its high energy density, portability, and high-cost performance, the

lithium-ion battery has been widely used in the field of new energy [7, 8]. Such as electric vehicles, aerospace, special robots, and other industries [9-12]. More and more attention has been paid to its health status. Accurate estimation of the state of charge (SOC) of lithium-ion batteries can greatly improve the performance and service life of lithium-ion batteries [13, 14]. Therefore, the real-time estimation of lithium-ion batteries plays an important role in its safety and usability.

Due to the wide use of lithium-ion batteries, the working environment is different. Its condition monitoring is easily affected by environmental noise [15]. Moreover, the internal chemical reaction of lithium-ion batteries is highly nonlinear, usually accompanied by polarization effect and ohmic effect. So the traditional algorithm is difficult to estimate the real-time SOC of lithium-ion batteries because of these factors [16-18]. Therefore, in the face of complex conditions, it is of great significance to use the reasonable and correct algorithm for real-time monitoring and safety control of the lithium-ion battery.

At present, the commonly used SOC estimation methods include the open-circuit voltage method (OCV) [19], ampere-hour integration method (Ah) [20, 21], neural network method (NN) [22], Kalman filtering method (KF) [23, 24], etc. The open-circuit voltage method takes a long time to stand the battery, which is not suitable for real-time estimation [25, 26]. Ampere-hour integration is a current integration method to estimate SOC [27]. Because the algorithm is simple, the anti-jamming ability is weak. If there is a deviation, with the passage of time, the error will be larger and larger, especially in the case of large external environmental interference. BP neural network has strong nonlinear approximation ability and can also be used for SOC estimation, but the disadvantage is that this method needs a large number of battery charge and discharge test data as the basis. If the detection error of voltage and current is too large, the estimation accuracy of SOC will be affected. If the algorithm only runs BP neural network, it will bring great burden to the running computer, and the calculation time is very long [28, 29]. As a typical prediction algorithm, the Kalman filtering is suitable for SOC estimation [30, 31], but it will inevitably produce errors in nonlinear processing, especially in the case of emergencies, which is easy to produce large errors and depends on the accurate battery model.

EKF algorithm only calculates the Jacobian matrix of the last time, and the noise is set to a fixed value, so it does not have good robustness in the face of emergencies, so an improved dynamic strategy algorithm is proposed. BP neural network is combined with extended Kalman filtering (BP-EKF) algorithm in the case of strong interference, strong noise and strong deformation. Based on the real-time and fast performance of EKF, the nonlinear processing characteristic of BP neural network is introduced to calculate the mutation events dynamically, so as to reasonably estimate the SOC of lithium-ion battery. The experimental results show that the method is effective and robust.

2.MATHEMATICAL ANALYSIS

In order to ensure a reasonable evaluation of the lithium-ion battery system, the appropriate model should be used to build the simulation environment of the battery, and the excellent algorithm should be used to estimate it.

2.1 First-order equivalent model

Considering the production application of lithium-ion battery, the first-order equivalent model is used to simulate lithium-ion battery. The first-order equivalent model has the characteristics of easy identification, few parameters and high accuracy. Its model structure is shown in Figure 1.

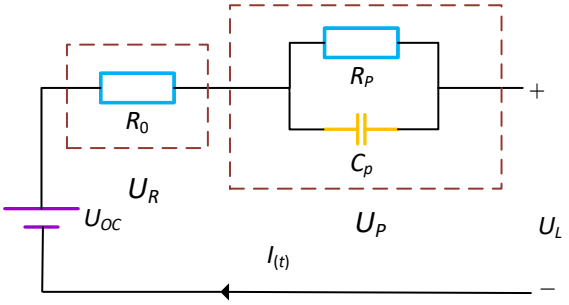

Figure 1. First-order RC electrical circuit model

In Figure 1, U_{OC} represents the open-circuit voltage, U_L is the terminal voltage, and R_0 represents the ohmic internal resistance. R_P and C_P represent the polarization effect of the lithium-ion battery. According to Kirchhoff's law and analyzing the model, the following equations can be obtained Eq. (1).

$$\begin{cases} U_{OC} = U_L - U_R - U_p \\ I(t) = C_p \dfrac{dU_p}{dt} + \dfrac{U_p}{R_p} \end{cases} \quad \textbf{(1)}$$

According to Eq. (1), using the knowledge of modern control theory, select state space variables, input variables and output variables for discretization, and obtain a discrete equation, as shown in Eq. (2).

$$\begin{cases} \begin{bmatrix} SOC_{k+1} \\ U_{P,k+1} \end{bmatrix} = \begin{bmatrix} 1 & 0 \\ 0 & e^{-\frac{\Delta t}{\tau}} \end{bmatrix} \begin{bmatrix} SOC_k \\ U_{L,k+1} \end{bmatrix} + \begin{bmatrix} -\dfrac{\Delta t}{Q_N} \\ R_P(1-e^{-\frac{T}{\tau}}) \end{bmatrix} I_k \\ U_{L,k} = U_{OC,k} - R_{0,k} I_k + \begin{bmatrix} 0 \\ -1 \end{bmatrix}^T \begin{bmatrix} SOC_k \\ U_{P,k} \end{bmatrix} \end{cases} \quad \textbf{(2)}$$

In Eq. (2), U_P represents the polarization voltage. Q_N is the rated capacity of the lithium-ion battery, and I_k is the current. Δt is the sampling time interval, and τ is called the time constant, $\tau = R_P C_P$.

2.2 Parameter identification

According to the experimental procedure, the Lithium-ion battery is tested by Hybrid Pulse Power Characterization test (HPPC). The HPPC test should be performed under SOC=1.0,0.9,0.8... etc.

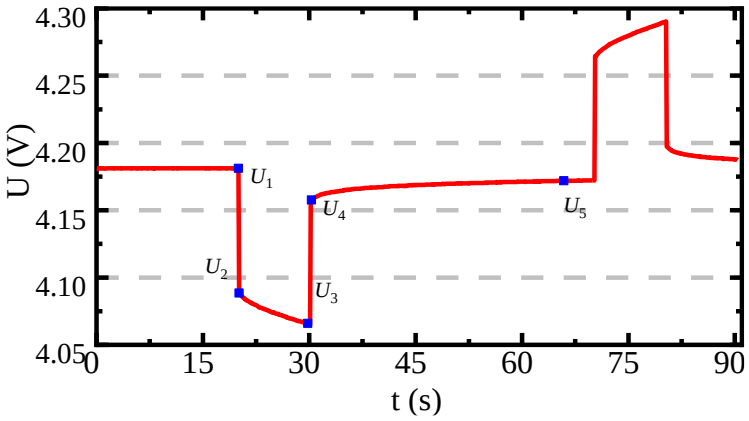

Figure 2. One-pulse experimental voltage curve

U_1-U_2 is the ohmic effect caused by R_0 in the model, which indicates the effect of rapid voltage drop at the instant of battery discharge. The same true for U_3-U_4. Eq. (3) can be obtained.

$$R_0 = \frac{(U_1 - U_2) + (U_4 - U_3)}{2I} \qquad (3)$$

The polarization capacitance C_P and the polarization capacitance R_P form RC ring, and the polarization effect appears, which indicates that the voltage of U_2-U_3 increases slowly. From this, the relevant parameters can be calculated, as shown in the following Eq. (4).

$$U_L = U_{OC} - IR_0 - IR_P e^{-\frac{t}{\tau}} \qquad (4)$$

In the equation, the time constant $\tau = R_P C_P$. By abstracting the above equation, the fitting curve can be easily obtained in MATLAB. The curve fitted by each point of HPPC can represent the related parameters of the first-order electrical circuit on each SOC, and its accuracy is also high.

2.3 Backpropagation network – extended Kalman filtering

The basic unit of BP neural network is artificial neuron, which is a multi input and single output nonlinear component.

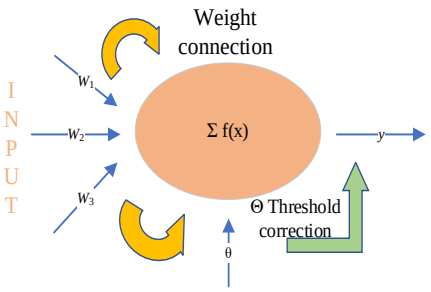

(a) Nerve unit

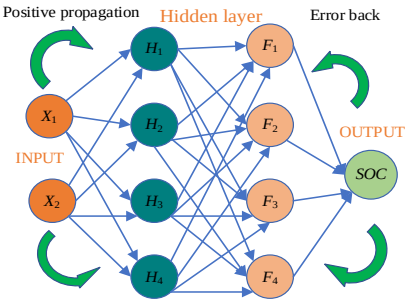

(b) Neural network structure diagram

Figure 3. BP neural network

The total structure is composed of input layer, hidden layer and output layer. The first stage is the signal forward propagation; The input information is processed layer by layer through the input layer and the hidden layer, and the actual output value of each unit is calculated; The second stage is the back propagation of the error. If the expected value does not match it, the error between the output value and the expected value will be calculated, so as to adjust the weight parameters between the layers. The schematic diagram is shown in Figure 3.

The error feedback is particularly important in BP neural network. The output error of the network can be expressed by the correlation function of the weight of the input layer V_{ij} and the weight of the hidden layer W_{JK}, as shown in Eq.(5).

$$\begin{cases} \Delta W_{jk} = -\eta \, \partial E / \partial W_{\mathrm{jk}} \\ \Delta V_{jk} = -\eta \, \partial E / \partial V_{ij} \end{cases} \tag{5}$$

The negative sign of the above formula is the direction of weight update, that is, the direction of gradient descent. E is the square of the error between the expected output and the actual output. From Eq.(6), we can see the weight update representation of hidden layer.

$$\begin{cases} W_{jk}(t+1) = W_{jk}(t) + \eta \delta_k y_j \\ W_{ij}(t+1) = W_{ij}(t) + \eta \delta_j x_i \end{cases} \tag{6}$$

In the above form η For learning efficiency, the range is (0,1). δ_k, δ_J is the error signal of output layer and hidden layer respectively. If the actual output of the neuron is larger than the expected output, the weights of all the connections with positive inputs are reduced and the weights of all the connections with negative inputs are increased; On the contrary, if the actual output of the neuron is smaller than the expected output, the weights of all the connections with positive inputs are increased and the weights of all the connections with negative inputs are decreased. The formula reflects the iterative process of network weight updating.

$$\begin{cases} jj = jX * jX \\ je = jX * E \\ dX = -(jj + I * mu) / je \end{cases} \tag{7}$$

Where JX is the Jacobian matrix of the performance of the deviation variable, E is all errors, I is the unit matrix. By using the Bayesian rule method, the correction function mu is introduced into the conventional mean square error. By setting the relevant weight parameters as random variables, the optimal weight function is determined according to the probability density of the weight.

The traditional BP network algorithm is optimized to minimize the linear combination of square error and weight, and the network obtained at the end of training will have good generalization ability.

$$mu = L_1 E + L_2 E_d \tag{8}$$

Where mu is the performance correction function; L_1 and L_2 are regularization parameters. E is all errors, E_d is the mean square error of network output; The network adjusts L_1 and L_2 adaptively. Bayesian regularization can effectively avoid over fitting of data, so that the data will not cause divergence and inaccuracy of output results due to the error of individual data.

because There may be a big gap in the order of magnitude of the input data, so the adjustment of the weight value will be seriously skewed during network training, so it can be solved by data normalization, as shown in Eq(9).

$$y = \frac{(y_{\max} - y_{\min}) * (x - x_{\min})}{(x_{\max} - x_{\min})} + y_{\min} \tag{9}$$

y is the normalized data, ymax and yman are parameters, set to 1 and - 1. x is the original data, x_{max} and x_{min} are the maximum and minimum values of the original data. The normalized data can avoid the error caused by the difference of input data magnitude, and improve the generalization ability of the network.

The extended Kalman filtering core is the update of covariance and Kalman gain. The Equation is as Eq.(10).

$$\begin{cases} \hat{P}_{k+1}^{-} = A_k \hat{P}_k A_k^T + Q_{k+1} \\ K_{k+1} = \hat{P}_{k+1}^{-} C_{k+1}^T \left(C_{k+1} \hat{P}_{k+1}^{-} C_{k+1}^T + R_{k+1} \right)^{-1} \end{cases} \tag{10}$$

In Eq.(10), there are noises Q and R in the update of covariance P and Kalman gain K. In practical applications, Q and R vary with the environment and the internal operating conditions of the battery. Because EKF uses local solution, it will bring the influence of the last prediction error to the next prediction. Therefore, under sudden events, using BP neural network to avoid the error caused by noise will be helpful to SOC estimation. The joint dynamic strategy of backpropagation neural network and extended Kalman filtering (BP-EKF) flowchart is Figure 4.

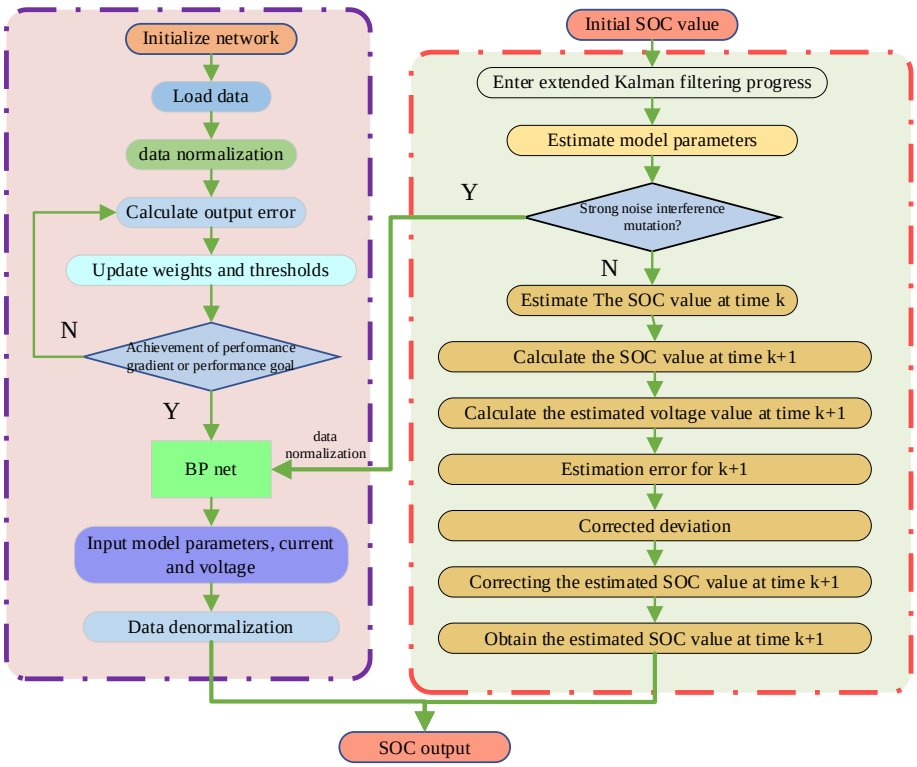

Figure 4. The joint dynamic strategy of backpropagation neural network and extended Kalman filtering flowchart

In Figure 4, to take into account the efficiency and accuracy of the algorithm, dynamic strategy planning is needed. The BP neural network is combined with the first-order circuit model to realize the five input one output mode which is driven by data and provided by the model.

First, the EKF program is used to calculate the first-order circuit parameters of SOC. When BP neural network is used for input and output under strong interference, the EKF program directly skips the update, avoids the influence of a lot of noise and deformation, and prevents the update of covariance P and Kalman gain K. Using the identification parameters of the first-order electrical circuit model, current and voltage, BP neural network can drive data more accurately and improve its ability to approach nonlinearity.

When the interference is weak, because the interference is small, the estimation accuracy will not have too big fluctuation. In order to improve the efficiency of the algorithm, the BP data network is not used, but directly into the estimation mode. The SOC value of the next time is estimated by the space state equation, covariance, and gain of the previous time.

3. EXPERIMENTAL RESULTS AND DISCUSSION

3.1 Parameter identification results and backpropagation net

The parameters of each SOC point are identified by curve fitting, and the data of ohmic resistance R_0, polarization resistance R_P, polarization capacitance C_P and open circuit voltage U_{OC} from 0.1 to 1 are obtained. The model parameters under different states of charge are shown in

Table 1.

Table 1. Model parameters under different SOC

SOC	R_0	R_P	C_P	U_{OC}
1.0	0.001851	0.0006286	13846.64333	4.17955
0.9	0.001894	0.0006478	12212.1025	4.0387
0.8	0.001872	0.0007028	11713.14741	3.9186
0.7	0.001876	0.0007502	11603.57238	3.8078
0.6	0.001879	0.0006082	13311.41072	3.69695
0.5	0.001913	0.0004946	16617.46866	3.63365
0.4	0.001916	0.0005284	17452.68736	3.5968
0.3	0.001947	0.000595	16060.5042	3.54735
0.2	0.002017	0.0007432	11469.32185	3.45585
0.1	0.002152	0.0007654	11411.02691	3.4656

Using Matlab/Simulink to verify, the real voltage and current data under the cycle discharge are imported in the first-order electrical circuit model. The model is verified by combining it with the parameter identification results. The estimation value is compared with the real value in

Figure 5.

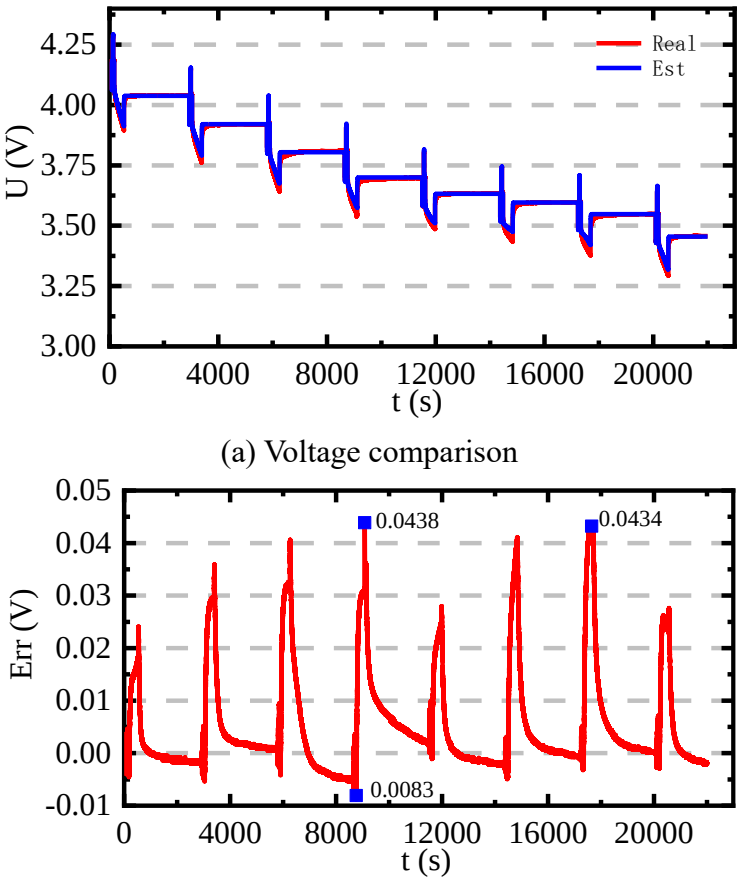

(a) Voltage comparison

(b) Estimation error

Figure 5. First-order electrical circuit model simulation results

In

Figure 5, the first-order electrical circuit model has a good tracking effect. The maximum estimated deviation is 0.4V, which can characterize the terminal voltage of the battery in operation.

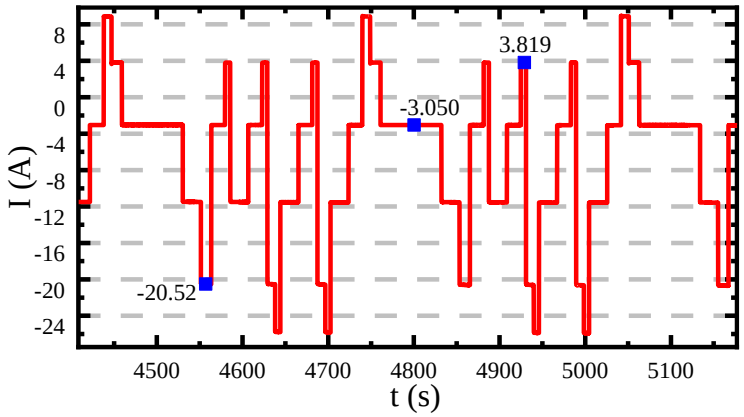

(a)Variation of current in BBDST

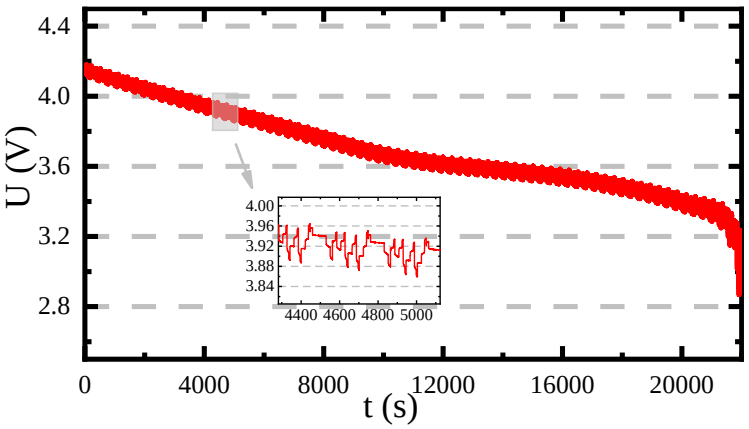

(b)Variation of voltage in BBDST

Figure 6. Current and voltage diagram of BBDST under training condition

For BP neural network, this experiment uses Beijing Bus Dynamic Stress Test (BBDST) for model training. BBDST condition is complex, which can reflect and better train data. There are 221488 groups of current and voltage, as shown in

Figure 6 below. Using the off-line EKF, the current and voltage at this time under BBDST condition are taken as input, and the first-order model parameters corresponding to SOC value at this time are added as input to form a five input model. The SOC obtained by the ampere-hour integration method is taken as the accurate output. The net model of BP neural network training can be obtained.

3.2 Capacity test and HPPC analysis

In order to verify the accuracy of the improved BP-EKF for SOC estimation of the lithium-ion battery, the capacity test experiment and the HPPC experiment are used to verify the estimation. Using the trained net model and the first-order electronic circuit model, and setting high interference points in the data, the interference points are separated by 100 groups of data. At the same time, the experiment uses the ampere-hour integration method and extended Kalman filtering algorithm as references, as shown in Figure 7.

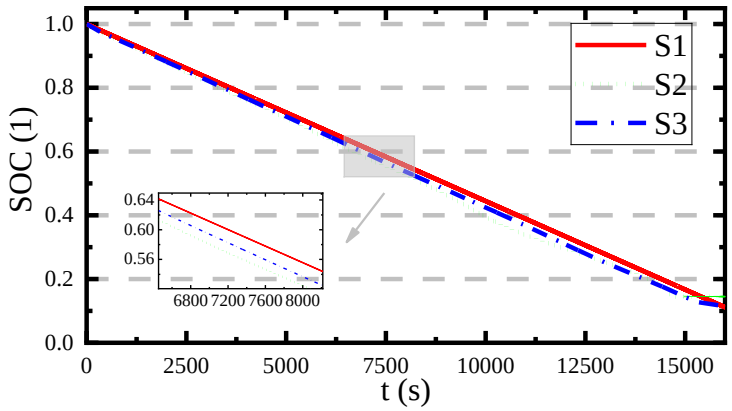

(a) SOC estimation in Capacity test

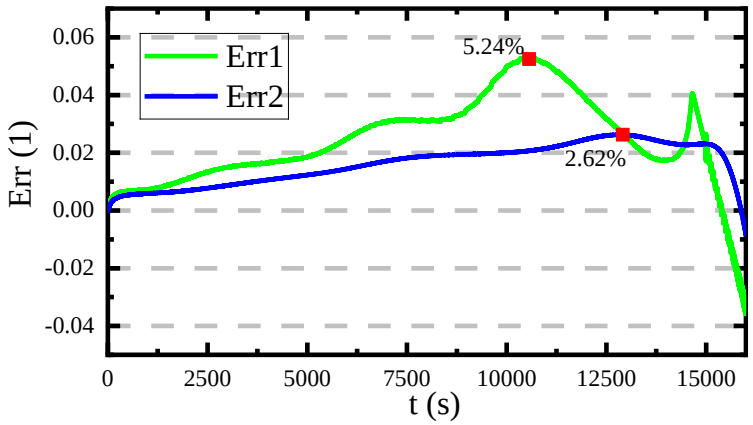

(b) SOC estimation errors in Capacity test

Figure 7. SOC estimation and error results in Capacity test

In Figure 7 (a), the S1 curve is the estimation of the ampere-hour integration method, the S2 curve is the estimation of extended Kalman filtering, and S3 is the estimation of BP-EKF. In Figure 7(b), the ampere-hour integration method is used as the reference value of accurate SOC. Err1 is the error of EKF and err2 is the error of BP-EKF. Because of the high interference point, the estimation results of the two algorithms are common, but the maximum error of the improved BP-EKF is 2.62%, and the maximum error of EKF is 5.24%. Compared with literature [32], this paper improves the numerical stability by improving the weight coefficient parameters, but there is always a nonlinear problem. BP algorithm is better than its algorithm in nonlinear problems, so its SOC estimation error is less than 3.51%, while the improved BP-EKF algorithm is less than 2.62%. Therefore, the improved BP-EKF algorithm has good results in the face of nonlinear problems.

In the HPPC experiment, there is a lot of standing time and burst current, and strong interference is set in the experiment, so it is necessary to estimate the SOC of the HPPC experiment. As shown in Figure 8.

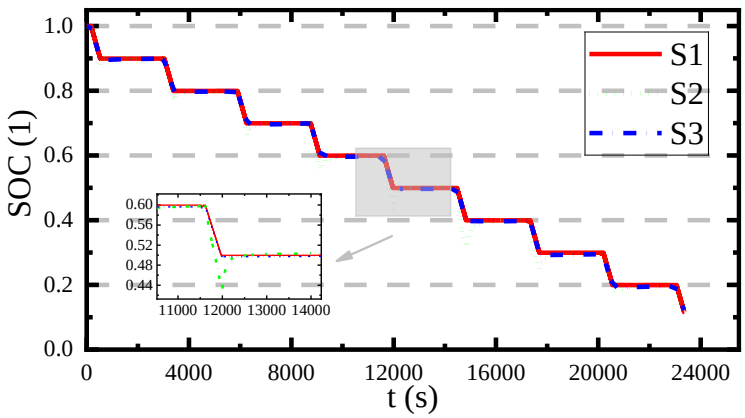

(a) SOC estimation in HPPC

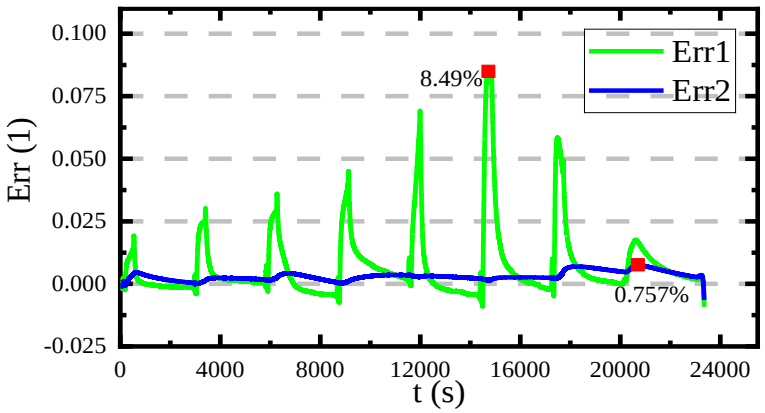

(b) SOC estimation errors in HPPC

Figure 8. SOC estimation and error results in HPPC

Similarly, the ampere-hour integration method and EKF algorithm are introduced. The significance of the curve is the same as that of the capacity test. S1 is ampere-hour integration, S2 is EKF, S3 is BP-EKF. Err1 is the error of the ampere-hour integration method and EKF, and err2 is the error of the ampere-hour integration method and BP-EKF. It can be seen from Figure 8 that when EKF encounters strong interference, the estimated SOC value will change abruptly, which will affect the next estimation accuracy and cause the butterfly effect. However, BP-EKF embodies the stability, and the maximum error is 0.757%, which is much smaller than the maximum error of 8.49% of EKF. Literature [33] proposes to use the iterative parameters of KF for BP training, which will complicate the on-line parameter estimation, and the accuracy is only about 2%. BP-EKF is not only faster than this method, but also the error reaches 0.757%, so BP-EKF algorithm is better.

3.3 Complex condition analysis

In practical applications, the real-time current of the lithium-ion battery is complex and changeable. In different working conditions, the current is often switched and stopped suddenly, which puts forward strict requirements on the dynamic performance of the battery and also brings difficulties to the SOC estimation of the lithium-ion battery under complex working conditions. To further verify the estimation model for SOC of the lithium-ion battery under more complex application conditions, the model is simulated and verified with self-defined DST experimental data. The current and voltage of DST are shown in Figure 9

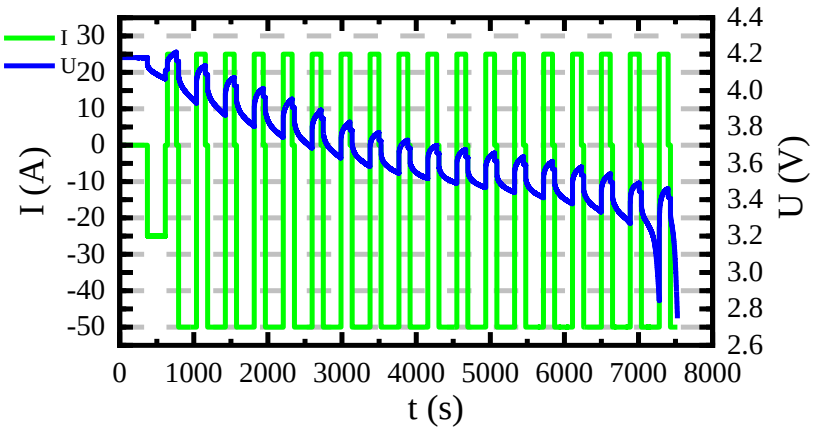

Figure 9. The current and voltage of DST

Considering the complex working condition of DST and the large variation of current and voltage, high-intensity interference is set every 50 points in the experiment to verify the anti-interference performance of the algorithm. And the ampere-hour integration method and extended Kalman filtering are introduced for comparison. SOC estimation under DST is shown in

Figure 10.

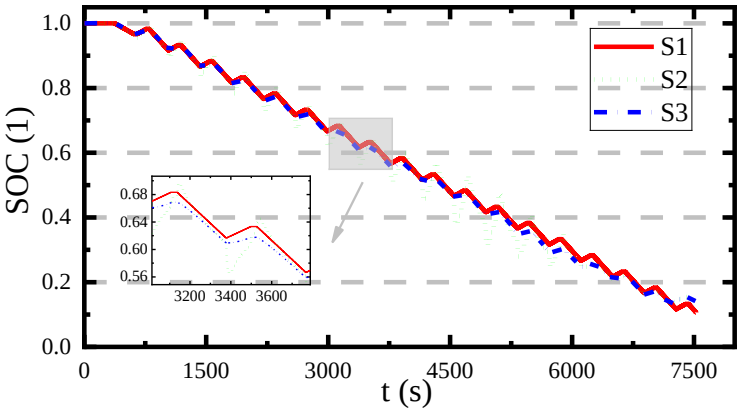

(a) SOC estimation in DST

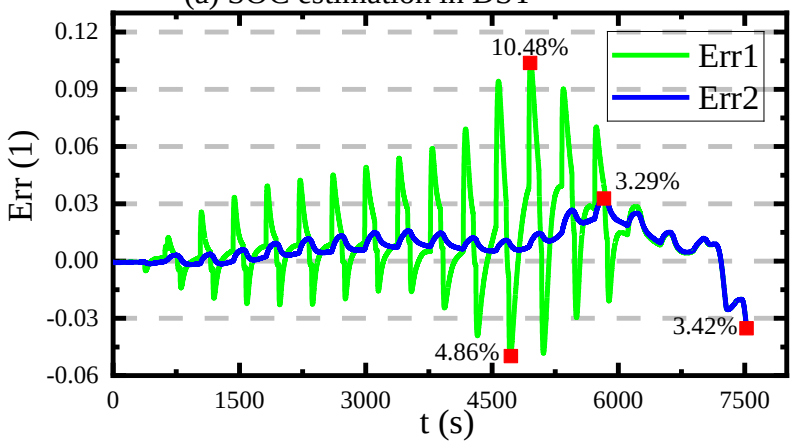

(b) SOC estimation errors in DST

Figure 10. SOC estimation and error results under DST test

S1 represents the ampere-hour integration method, S2 represents EKF and S3 represents BP-EKF. Err1 represents the error between the ampere-hour integration method and EKF, and err2 represents the error between the ampere-hour integration method and BP-EKF. From

Figure 10, the complex working conditions and strong interference make the EKF estimation difficult, and the maximum error is 10.48% and unstable. However, the maximum error of the BP-EKF algorithm is 3.42%, which shows a good tracking effect, and it can also estimate SOC value well in the face of strong interference. Compared with the related literature [34], the EKF algorithm in this literature does not perform well in the face of current noise and different temperatures, and even has an error of 10% at the beginning. Therefore, the improved BP-EKF can stabilize the error and perform well in the initial stage of estimation.

The real-time monitoring of the battery is very important, so the estimation speed is also an excellent embodiment of the algorithm. According to the working conditions of the capacity test, HPPC and DST, the calculation time is compared (excluding the time of BBDST training net), as shown in

Table 2 below.

Table 2. Running time of each algorithm

Conditions(data) / Algorithms	Capacity (160000)	HPPC (233574)	DST (75261)
EKF	24.549971s	39.780623s	10.043536s
BP	1349.731788s	2404.429559s	684.297572s
BP-EKF	28.879908s	45.005655s	14.464077s

In

Table 2, the speed of EKF is the fastest, that of BP is the slowest, and that of BP-EKF is medium. But the accuracy of EKF is not high, so BP-EKF shows the characteristics of high speed and high accuracy. It is verified that BP-EKF improves SOC estimation of the lithium-ion battery under high interference.

4.CONCLUSIONS

It is very important and difficult to accurately estimate the SOC of lithium-ion batteries in different environments. In this paper, the first-order electrical circuit model is used to characterize the state and output characteristics of the lithium-ion battery, and the HPPC experiment is used to identify the parameters. The extended Kalman filtering algorithm is used for fast estimation, and BP neural network is used to reduce the influence of strong interference on SOC estimation. The results show that the improved dynamic strategy joint algorithm BP-EKF has a good estimation effect. Under the set indirect strong interference, the average error can be controlled within 1.609% and the maximum error

can be controlled within 3.291% under different working conditions. It is verified that the improved BP-EKF algorithm is helpful to the SOC estimation accuracy of the lithium-ion battery.

ACKNOWLEDGMENTS
The work was supported by National Natural Science Foundation of China (No. 61801407), Sichuan s cience and technology program (No. 20019YFG0427), China Scholarship Council (No. 201908515099) and Fund of Robot Technology Used for Special Environment Key Laboratory of Sichuan Province (No. 18kftk03), Natural Science Foundation of and Southwest University of Science and Technology(No.17zx7110,18zx7145).

References

1. M. A. Khan, I. Al-Shankiti, A. Ziani and H. Idriss, *Sustainable Energy Fuels*, 5 (2021) 1085.
2. Z. L. Du, B. Q. Lin and C. X. Guan, *Resour. Conserv. Recy*, 143 (2019) 17.
3. C. Raghutla, M. Shahbaz, K. R. Chittedi and Z. L. Jiao, *Renew. Energy*, 169 (2021) 231.
4. S. Cheng, G. J. Zhao, M. Gao, Y. T. Shi, M. M. Huang and M. Marefati, *Int. J. Hydrogen Energy*, 46 (2021) 8048.
5. Y. Han, H. C. Zhang and Z. Y. Hu, *Appl. Therm. Eng.*, 185 (2021) 116417.
6. C. Y. Chen, A. H. Liang, C. L. Huang, T. H. Hsu and Y. Y. Li, *J .Alloy. Compd.*, 844 (2020) 156025.
7. J. M. Collins and D. McLarty, *Appl. Energy*, 265 (2020) 114787.
8. S. Dorfler, S. Walus, J. Locke, A. Fotouhi, D. J. Auger, N. Shateri, T. Abendroth, P. Hartel, H. Althues and S. Kaskel, *Energy Technol-Ger*, 9 (2020) 2000694.
9. X. F. Ding, D. H. Zhang, J. W. Cheng, B. B. Wang and P. C. K. Luk, *Appl. Energy*, 254 (2019) 113615.
10. D. F. Finger, C. Braun and C. Bil, *J. Aerospace Eng.*, 33 (2020) 04020007.
11. P. Taus, M. Tausova, P. Sivak, M. S. Muchova and E. Mihalikova, *Energies*, 13 (2020) 4497.
12. C. E. D. Riboldi, L. Trainelli and F. Biondani, *J. Aerospace Eng.*, 33 (2020) 04020031.
13. Y. B. Rao, *Sustain. Comput-Infor.*, 27 (2020) 100396.
14. R. Methekar, *J. Renew. Sustainable Energy*, 10 (2018) 64103.
15. F. Maletic, M. Hrgetic and J. Deur, *Energies*, 13 (2020) 540.
16. J. Xie and T. Yao, *Ieee T. Transp. Electr.*, 7 (2021) 1.
17. J. L. Xie, Z. C. Li, J. F. Jiao and X. Y. Li, *Measurement*, 173 (2021) 108567.
18. M. S. El Din, A. A. Hussein and M. F. Abdel-Hafez, *Ieee T. Transp. Electr.*, 4 (2018) 408.
19. L. L. Li, Z. F. Liu and C. H. Wang, *J. Test Eva.l*, 48 (2020) 1712.
20. Z. X. Liu, Z. Li, J. B. Zhang, L. S. Su and H. Ge, *Energies*, 12 (2019) 757.
21. X. Xiong, S. L. Wang, C. Fernandez, C. M. Yu, C. Y. Zou and C. Jiang, *Int. J. Energ. Res.*, 44 (2020) 11385.
22. Z. Wu, M. Shang, D. Shen and S. Qi, *J. Renew. Sustain. Ener.*, 11 (2019) 24103.
23. L. Feng, J. Ding and Y. Y. Han, *Ionics*, 26 (2020) 2875.
24. M. Gholizadeh and A. Yazdizadeh, *Iet Electr. Syst. Tran.*, 10 (2020) 135.
25. J. Meng, M. Boukhnifer and D. Diallo, *Iet Electr. Syst. Tran.*, 10 (2020) 162.
26. G. Q. Jin, L. Li, Y. D. Xu, M. H. Hu, C. Y. Fu and D. T. Qin, *Energies*, 13 (2020) 1785.
27. X. Lai, D. D. Qiao, Y. J. Zheng and L. Zhou, *Appl. Sci-Basel*, 8 (2018) 2028.
28. J. Renteria-Cedano, J. Rivera, F. Sandoval-Ibarra, S. Ortega-Cisneros and R. Loo-Yau, *Electronics-Switz*, 8 (2019) 761.
29. M. Jiao, D. Q. Wang and J. L. Qiu, *J. Power Sources*, 459 (2020) 228051.

30. W. D. Wang, X. T. Wang, C. L. Xiang, C. Wei and Y. L. Zhao, *Ieee Access*, 6 (2018) 35957.
31. X. F. Tang, Q. C. Zhang and L. Hu, *Ieee Access*, 8 (2020) 62261.
32. S. L. Wang, C. Fernandez, Z. W. Xie, X. X. Li, C. Y. Lou and Q. Li, *Energy Sci. Eng.*, 7 (2019) 3038.
33. W. Z. Zhao, X. C. Kong and C. Y. Wang, *P I Mech Eng D-J Aut*, 232 (2018) 357.
34. D. Y. Cui, B. Z. Xia, R. F. Zhang, Z. Sun, Z. Z. Lao, W. Wang, W. Sun, Y. Z. Lai and M. W. Wang, *Energies*, 11 (2018) 995.